



## **Analysis of the major chiral compounds of Artemisia herba-alba essential oils (EOs) using reconstructed vibrational circular dichroism (VCD) spectra: En route to a VCD chiral signature of EOs**

Mohammed El-Amin Said, Pierre Vanloot, Isabelle Bombarda, Jean-Valère Naubron, El Montassir Dahmane, Ahmed Aamouche, Marion Jean, Nicolas Vanthuyne, Nathalie Dupuy, Christian Roussel

### **► To cite this version:**

Mohammed El-Amin Said, Pierre Vanloot, Isabelle Bombarda, Jean-Valère Naubron, El Montassir Dahmane, et al.. Analysis of the major chiral compounds of Artemisia herba-alba essential oils (EOs) using reconstructed vibrational circular dichroism (VCD) spectra: En route to a VCD chiral signature of EOs. *Analytica Chimica Acta*, 2016, 903, pp.121-130. 10.1016/j.aca.2015.11.010 . hal-01441883

**HAL Id: hal-01441883**

**<https://hal.science/hal-01441883>**

Submitted on 12 Apr 2018

**HAL** is a multi-disciplinary open access archive for the deposit and dissemination of scientific research documents, whether they are published or not. The documents may come from teaching and research institutions in France or abroad, or from public or private research centers.

L'archive ouverte pluridisciplinaire **HAL**, est destinée au dépôt et à la diffusion de documents scientifiques de niveau recherche, publiés ou non, émanant des établissements d'enseignement et de recherche français ou étrangers, des laboratoires publics ou privés.

# Analysis of the major chiral compounds of *Artemisia herba-alba* essential oils (EOs) using reconstructed vibrational circular dichroism (VCD) spectra: En route to a VCD chiral signature of EOs

Mohammed El-Amin Said <sup>a</sup>, Pierre Vanloot <sup>a</sup>, Isabelle Bombarda <sup>a</sup>, Jean-Valère Naubron <sup>b</sup>, El Montassir Dahmane <sup>d</sup>, Ahmed Aamouche <sup>d</sup>, Marion Jean <sup>c</sup>, Nicolas Vanthuyne <sup>c</sup>, Nathalie Dupuy <sup>a, \*\*</sup>, Christian Roussel <sup>c, \*</sup>

<sup>a</sup> Aix-Marseille Université, EA4672 LISA Equipe METICA, Case 451, Av. Escadrille Normandie Niemen, 13397 Marseille Cedex 20, France

<sup>b</sup> Aix-Marseille Université, Spectropole, Service 511, F-13397 Marseille, France

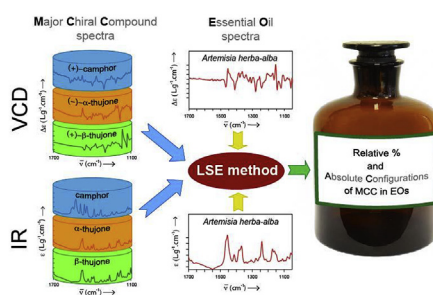
<sup>c</sup> Aix-Marseille Université, Centrale Marseille, CNRS, ISM2 UMR 7313, Marseille, France

<sup>d</sup> MSISM Research Team Faculte Polydisciplinaire, Cadi Ayyad University, Safi, Morocco

## HIGHLIGHTS

- The IR/VCD spectra of crude EO were modeled as a linear weighted combination of the individual spectra of pure enantiomers.
- The relative percentage and absolute configuration of the major chiral compounds of EOs are obtained combining VCD and LSE.
- Comparing IR-LSE and VCD-LSE reveals the occurrence as a single or a mixture of enantiomers of each major chiral compound.

## GRAPHICAL ABSTRACT



## ABSTRACT

An unprecedented methodology was developed to simultaneously assign the relative percentages of the major chiral compounds and their prevailing enantiomeric form in crude essential oils (EOs). In a first step the infrared (IR) and vibrational circular dichroism (VCD) spectra of the crude essential oils were recorded and in a second step they were modeled as a linear weighted combination of the IR and VCD spectra of the individual spectra of pure enantiomer of the major chiral compounds present in the EOs. The VCD spectra of enantiomer of known enantiomeric excess shall be recorded if they are not yet available in a library of VCD spectra. For IR, the spectra of pure enantiomer or racemic mixture can be used. The full spectra modelizations were performed using a well known and powerful mathematical model (least square estimation: LSE) which resulted in a weighting of each contributing compound. For VCD modelization, the absolute value of each weighting represented the percentage of the associate compound while the attached sign addressed the correctness of the enantiomeric form used to build the model. As an example, a model built with the non-prevailing enantiomer will show a negative sign of the weighting value. For IR spectra modelization, the absolute value of each weighting represented the percentage of the compounds without of course accounting for the chirality of the prevailing enantiomers. Comparison of the weighting values issuing from IR and VCD spectra modelizations is a valuable

### Keywords:

*Artemisia herba-alba*  
Essential oil  
Vibrational circular dichroism  
Chiral signature  
Diastereomers

\* Corresponding author.

\*\* Corresponding author.

E-mail addresses: [nathalie.dupuy@univ-amu.fr](mailto:nathalie.dupuy@univ-amu.fr) (N. Dupuy), [christian.roussel@univ-amu.fr](mailto:christian.roussel@univ-amu.fr) (C. Roussel).

source of information: if they are identical, the EOs are composed of nearly pure enantiomers, if they are different the chiral compounds of the EOs are not in an optically pure form. The method was applied on four samples of essential oil of *Artemisia herba-alba* in which the three major compounds namely (–)- $\alpha$ -thujone, (+)- $\beta$ -thujone and (–)-camphor were found in different proportions as determined by GC–MS and chiral HPLC using polarimetric detector. In order to validate the methodology, the modelization of the VCD spectra was performed on purpose using the individual VCD spectra of (–)- $\alpha$ -thujone, (+)- $\beta$ -thujone and (+)-camphor instead of (–)-camphor. During this work, the absolute configurations of (–)- $\alpha$ -thujone and (+)- $\beta$ -thujone were confirmed by comparison of experimental and calculated VCD spectra as being (1*S*,4*R*,5*R*) and (1*S*,4*S*,5*R*) respectively.

## 1. Introduction

*Artemisia herba-alba* (AHA) is a species belonging to the Asteraceae family. It grows in arid and semi-arid climates around Mediterranean Sea. It is characteristic of the steppes and Middle East deserts (Egypt and Sinai desert), North Africa (Algeria, Tunisia and Morocco), Spain, with extension into Northwestern Himalayas [1–4]. Essential oil (EO) obtained by steam distillation of the aerial parts of the plant is widely used in folk medicine to treat diabetes, bronchitis and other diseases such as jaundice [5], and in pharmaceutical industries [6–8]. *A. herba-alba* essential oil (AHA-EO) is a yellow oil with a strong penetrating pleasant herbaceous odor characteristic of the plant. Various studies reporting on the chemical composition of AHA-EO from different origins revealed the existence of different chemotypes (CT) such as camphor CT, and thujones CT [9]. Chiral components in plants usually exist as one largely predominant optical isomer. In addition, the inspection of enantiomeric ratios could characterize regional differences between essential oils [10]. The presence of scalemic or racemic pairs (one-to-one ratios of each enantiomer) most often indicates an unnatural origin or is the result of partial or total racemization during the processing. Interestingly, (+) or (–)-camphor may be found in natural sources in association with (–)- $\alpha$ -thujone and/or (+)- $\beta$ -thujone diastereoisomers [11], while the enantiomers of the respective thujones have not been detected [10–12]. In a previous work, (–)- $\alpha$ -thujone and (+)- $\beta$ -thujone epimers were separated from camphor enantiomers by enantioselective HPLC with polarimetric detection [10]. Spectroscopic methods should be also useful for crude essential oils analysis. Molecular spectroscopy techniques such as mid-infrared (MID-IR) allowed the differentiation of essential oils such as essential oil of thyme, oregano and chamomile [13] or the quantitative analysis of the major constituent in essential oil of lavandin Grosso [14]. However these techniques are not suitable to address the chiral issues in EOs, instead spectroscopic methods based on electronic circular dichroism (ECD) or vibrational circular dichroism (VCD) shall be used. Generally, these methods that measure the differential absorption of left and right circularly polarized lights are carried on to compare experimental and theoretical spectra in order to elucidate the absolute configuration of optically pure chiral molecules [15]. The efficiency of these techniques is largely demonstrated in the literature through the high growing number of absolute configuration determinations [16–21]. In the case of natural products, the vibrational circular dichroism (VCD) are most often performed on pure isolated compounds [22–24]. IR as well as VCD spectroscopies are both quantitative techniques, the regression methods (LSE, PLS) are already widely used in IR spectroscopy to quantify the major constituents in complex mixtures while they have not yet been applied in VCD spectroscopy of chiral complex mixtures [14,25,26]. Our purpose was introducing the Least Square Estimation (LSE) method in VCD spectra treatment of complex mixture of chiral compounds [27].

The VCD spectra were recorded for optically pure (+)-camphor, (–)- $\alpha$ -thujone, (+)- $\beta$ -thujone as reference compounds and crude AHA-EOs. A reconstruction method based on (LSE) was developed in order to assign the prevailing enantiomeric form and the relative percentage of chiral compounds in four samples of AHA-EO from Algeria and Morocco. For comparison and validation purposes, the chemical composition of these four samples was also determined by GC coupled to mass spectrometry and the prevailing enantiomeric forms were determined for the major chiral compounds through the optical rotation sign (ORS) acquired by an online Jasco polarimetric detector during enantioselective HPLC of crude EOs.

## 2. Experimental section

### 2.1. Samples

Samples 1 and 4 of AHA aerial part were collected during April 2013 and 2014 at the flowering stage from the region of Beni Ounif, 110 km in the North of Bechar in the south-west of Algeria (latitude: 32° 1' 25" N; longitude: 1° 35' 40" W; altitude: 970.5 m); Specimens were then dried in the open air for fifteen days and were conserved into freshness conditions before EO extraction. Sample 2 of AHA aerial part was collected at the flowering stage on July 2010, from the Atlas Mountains, near Marrakech (Morocco) and dried at room temperature for ten days before EO extraction. Dried leaves of AHA were subjected to hydrodistillation for 6 h. The EOs obtained were dried over anhydrous sodium sulfate, filtered and stored in a sealed vial in the dark at 4 °C before analysis. The oil yields were 1.89%, 2.57%, 2.35% for EOs 1, 2 and 4 respectively. Sample 3 of AHA is a commercial EO from Morocco origin purchased from Natur-ources (Sherbrooke, Canada).

### 2.2. Chemicals

The pure (–)- $\alpha$ -thujone and (+)- $\beta$ -thujone were obtained from a commercially  $\alpha$ , $\beta$ -thujone mixture (~70%, ~10% respectively) (89230) from Sigma–Aldrich (Steinheim, Germany) after semi-preparative chromatography over Chiralpak AZ-H from Chiral Technologie Europe (Illkirch, France), with a 99:1 hexane/2-PrOH mixture as the mobile phase [10]. Approximately 80 mg of pure (–)- $\alpha$ -thujone and 20 mg of pure (+)- $\beta$ -thujone were obtained from 200 mg of commercially mixture. (+)-Camphor (A10708) was purchased from Alfa Aesar (Karlsruhe, Germany).

### 2.3. Chiral HPLC

The analytical chromatography analyses of the AHA-EOs were performed on a Lachrom-Elite unit, Hitachi High-Technologies (California, USA), composed of a L-2130 pump, a L-2130 autosampler, a L-2350 oven and a L-2455 DAD-detector. The semi-preparative chromatography analyses were performed on a

Knauer unit with pump, TCI-MBS column from Tokyo Chemical Industry (Antwerp, Belgium), a mobile phase composed of a mixture of 1% v/v of 2-PrOH in hexane at 1 ml min<sup>-1</sup>, UV detector and software to collect the different fractions. The separations were monitored by a JASCO OR-1590 online polarimeter detector (Bouguenais, France). 1 mg of each sample was diluted in 1 ml of the mobile phase (99:1 v/v hexane/2-PrOH) before injection.

#### 2.4. GC/MS analysis

An Agilent Technologies GC instrument (Utilis, France), equipped with a GC 7890A gas chromatograph system, a MS 5975C VL MSD mass spectrometer detector and a HP-5MS capillary column J&W Scientific (30 m × 0.25 mm; film thickness 0.25 μm) was used. The data acquisition and processing were performed using the MSD ChemStation (Agilent) software. 1 μl of diluted EO (0.05 g in 1.5 ml of CH<sub>2</sub>Cl<sub>2</sub>) was injected. The experimental conditions were: solvent delay, 2 min; column temperature program, 2 min at 80 °C, then 80–200 °C (5 °C/min), then 200–260 °C (20 °C/min), and held at final temperature for 5 min; injector (split ratio 60) and detector temperatures were 250 °C; carrier gas was helium at a flow rate of 1.2 ml min<sup>-1</sup>; ionization voltage 70 eV; electron multiplier, 1 kV. The identification of the compounds was based on the comparison of their mass spectra with those of Wiley and NIST libraries as well as by comparison of their retention indices with those of authentic samples. EOs compositions were given as relative area percentages and for peak accounting for more than 0.1%.

#### 2.5. VCD spectroscopy

IR and VCD spectra were collected on a Vertex70 Fourier transform infrared spectrometer coupled with PMA 50 accessory, Bruker Corporation (Ettlingen, Germany). The VCD spectra were recorded with CaF<sub>2</sub> windows with a constant path length (200 μm) for 3 h at 4 cm<sup>-1</sup> resolution and room temperature. Each sample was diluted in the CCl<sub>4</sub> solvent for best solubility and weak absorption in the region of interest. The concentration of each sample was: (–)-α-thujone (137 g L<sup>-1</sup>), (+)-β-thujone (137 g L<sup>-1</sup>), (+)-camphor (137 g L<sup>-1</sup>), EO1 (99 g L<sup>-1</sup>), EO2 (110 g L<sup>-1</sup>), EO3 (111 g L<sup>-1</sup>) and EO4 (130 g L<sup>-1</sup>). The baseline of the VCD and IR spectra were corrected with the corresponding spectrum of the solvent obtained under the same experimental conditions. Spectra were collected in the MID-IR region, 1500–1050 cm<sup>-1</sup>. Calculations were performed on the (1S,4R,5R) and (1S,4S,5R) diastereomers of α-thujone and β-thujone respectively. The geometry optimizations, vibrational frequencies, IR absorption and VCD intensities were calculated with Density Functional Theory (DFT) using B3LYP functional combined with 6-311 + G(d,p) basis set. The average effects of the solvent were modeled using the implicit solvation model SMD. Computed harmonic frequencies are generally larger than the fundamentals observed experimentally. They have been calibrated using a scaling factor of 0.98. IR absorption and VCD spectra were constructed from calculated dipole and rotational strengths assuming Lorentzian band shape with a half-width at half maximum of 8 cm<sup>-1</sup>.

#### 2.6. Spectral reconstruction and prediction

The VCD spectrum of a chiral compound ΔA( $\bar{\nu}_i$ ) is defined assuming Beer–Lambert's law, eq. (1).

$$\Delta A(\bar{\nu}_i) = (ee)IC\Delta\epsilon(\bar{\nu}_i) \quad (1)$$

ΔA( $\bar{\nu}_i$ ) and Δε( $\bar{\nu}_i$ ) are the VCD spectrum defined in terms of absorbances and molar absorptivities respectively. C is the concentration

of the sample being measured and l is the path length. (ee) is the enantiomeric excess of the sample introduced to correct for deviation of the chiral sample from the pure major enantiomer of the chiral molecule being measured ( $ee = (C_{Major} - C_{minor}) / (C_{Major} + C_{minor})$  with  $C_{Major}$  and  $C_{minor}$  the concentrations of major and minor enantiomers respectively). eq. (1) breaks down if intermolecular interactions between solute molecules reach a significant level. They have been avoided using sufficiently low levels of concentration. The VCD spectra of EOs ΔA<sub>EO</sub>( $\bar{\nu}_i$ ) were measured and reconstructed as a weighted combination of pure spectra of the chiral compounds ΔA<sub>k</sub>( $\bar{\nu}_i$ ) (k refers to a chiral compound) using additive property of the Beer–Lambert law, eq. (2). All spectra were given in molar absorptivity Δε( $\bar{\nu}_i$ ), to be free on the choice of sampling (concentration C and path length l), eq. (3).

$$\Delta A_{EO}(\bar{\nu}_i) = \sum_k \Delta A_k(\bar{\nu}_i) \quad (2)$$

$$\Delta\epsilon_{EO}(\bar{\nu}_i) = \sum_k x_k(ee)_k \Delta\epsilon_k(\bar{\nu}_i) \quad (3)$$

$x_k = C_k/C_{EO}$  and  $(ee)_k$  are respectively the molar fraction and the enantiomeric excess of the chiral molecule k in the EO. The path length l has been kept constant for all measurements (200 μm). The contribution of a chiral molecule to Δε<sub>EO</sub>( $\bar{\nu}_i$ ) depends of its molar fraction or/and its enantiomeric excess in the EO, eq. (4).

$$\Delta\epsilon_{EO}(\bar{\nu}_i) = \sum_{k'}^{Major} x_{k'}(ee)_{k'} \Delta\epsilon_{k'}(\bar{\nu}_i) + \sum_{k''}^{minor} x_{k''}(ee)_{k''} \Delta\epsilon_{k''}(\bar{\nu}_i) \quad (4)$$

$\sum_{k'}^{Major} x_{k'}(ee)_{k'} \Delta\epsilon_{k'}(\bar{\nu}_i)$  are the contributions of the major chiral molecules which represent more than 5% of the total relative composition with an enantiomeric excess greater than 80%.

$\sum_{k''}^{minor} x_{k''}(ee)_{k''} \Delta\epsilon_{k''}(\bar{\nu}_i)$  are the contributions of minor chiral molecules which represents less than 5% of the total relative composition. We consider them minor because they are of the same intensities of the baseline artifacts. The value of the molar fractions  $x_{k'}$  was predicted using a Least Square Estimation (LSE). In the case of VCD spectra, the sign of  $x_{k'}$  also provided access to the prevailing enantiomeric form. A positive sign means that the proper enantiomer was used to build the model while a negative sign indicates that the opposite enantiomer is actually present in the crude EO. Moreover, eq. (4) must be completed in order to take into account the artifacts of measure  $a(\bar{\nu}_i)$  and the so called matrix effects  $M(\bar{\nu}_i)$  which are the effects on the VCD spectra of all molecules, chiral and achiral, that compose the EOs (eq. (5)). Indeed these effects are not present in the spectra of the isolated molecules that are used in the reconstruction.

$$\Delta\epsilon_{EO}(\bar{\nu}_i) = \sum_{k'}^{Major} x_{k'}(ee)_{k'} \Delta\epsilon_{k'}(\bar{\nu}_i) + B(\bar{\nu}_i) \quad (5)$$

with  $B(\bar{\nu}_i) = \sum_{k''}^{minor} x_{k''}(ee)_{k''} \Delta\epsilon_{k''}(\bar{\nu}_i) + M(\bar{\nu}_i) + a(\bar{\nu}_i)$

This equation can be written in matrix form as:

$$\Delta E_{EO} = X\Delta E_k + B \quad (6)$$

X is the vector of unknown parameters, eq. (7), ΔE<sub>EO</sub> and ΔE<sub>k</sub> contain the VCD spectra of the EO and the major chiral compounds, eqs. (8) and (9) respectively, and B is the intercept of the model.

$$X = \begin{bmatrix} x_1(ee_1) \\ x_2(ee_2) \\ \vdots \\ x_n(ee_n) \end{bmatrix} = \begin{bmatrix} x_1 \\ x_2 \\ \vdots \\ x_n \end{bmatrix} [(ee_1) \quad (ee_2) \quad \dots \quad (ee_n)] \quad (7)$$

$$\Delta E_{EO} = \begin{bmatrix} \Delta \varepsilon_{EO}(\bar{\nu}_1) \\ \Delta \varepsilon_{EO}(\bar{\nu}_2) \\ \vdots \\ \Delta \varepsilon_{EO}(\bar{\nu}_n) \end{bmatrix} \quad (8)$$

$$\Delta E_k = \begin{bmatrix} \Delta \varepsilon_1(\bar{\nu}_1) & \Delta \varepsilon_2(\bar{\nu}_1) & \dots & \Delta \varepsilon_k(\bar{\nu}_1) \\ \Delta \varepsilon_1(\bar{\nu}_2) & \Delta \varepsilon_2(\bar{\nu}_2) & \dots & \Delta \varepsilon_k(\bar{\nu}_2) \\ \vdots & \vdots & \ddots & \vdots \\ \Delta \varepsilon_1(\bar{\nu}_n) & \Delta \varepsilon_2(\bar{\nu}_n) & \dots & \Delta \varepsilon_k(\bar{\nu}_n) \end{bmatrix} \quad (9)$$

where each column of  $\Delta E_k$  or  $\Delta E_{EO}$  contains the absorptivities at  $\bar{\nu}_n$  wavenumbers and each line of  $\Delta E_k$ , the absorptivities of the  $k$  major chiral compounds.

The least squares estimators of the unknown parameters  $B$  and  $X$  (eqs (10) and (11)) are:

$$\hat{B} = \bar{E}_{EO} \quad (10)$$

$$\hat{X} = (E_k^T E_k)^{-1} E_{EO}^T E_k^T \quad (11)$$

At the end, the value and the sign of the  $x$ -coefficients allows us to know relative percentage of the major chiral compounds in the mixture and their prevailing enantiomeric form, respectively. The same model was developed using normal IR spectra. The equations are given in [Supplementary Materiel](#). The models were built using full cross validation method during the calibration developments and the solvent spectra were substracted in each case. The chemometric calculations were performed using the Unscrambler X (v10.3, CAMO software, Oslo, Norway) software.

### 3. Results and discussion

#### 3.1. GC-MS

The chemical compositions of the oils were investigated using GC/MS technique ([Table S-1](#)). Forty-three compounds were identified, representing 98.3%, 99.7%, 94.4% and 99.5% of the oil for the EOs 1, 2, 3 and 4 respectively. The major compounds were oxygenated monoterpenes including  $\alpha$ -thujone,  $\beta$ -thujone and camphor. The sesquiterpenes like  $\alpha$ -amorphene, germacrene-D, bicyclogermacrene,  $\delta$ -cadinene,  $\beta$ -caryophyllene and  $\alpha$ -cubebene were found in smaller amounts. It was interesting to note that the chiral compounds represent 93.8%, 94.4%, 82.3% and 94.6% of the total composition for the EOs 1, 2, 3 and 4 respectively. In this work only the major chiral constituents were taken into account, *ie*  $\alpha$ -thujone,  $\beta$ -thujone and camphor. These three compounds contribute for 78.9%, 78.0%, 60.8% and 82.7% of the total composition of the EOs 1, 2, 3 and 4 respectively. EOs 1, 2 and 4 contain  $\alpha$ -thujone as major compound (57.4%, 35.4%, and 58.2% respectively) so they are  $\alpha$ -thujone CT. Our results are in agreement with those previously reported by Mighri et al. and Derwich et al. in which  $\alpha$ -thujone is the major compound (49 and 42% respectively) in *AHA*-EOs from Tunisian and Moroccan origin respectively [3,7]. EO3 is a camphor CT since camphor is the major compound (34.5%). This result was reported previously by Vernin et al. in which camphor is the major compound (48%) in *AHA*-EOs from Algerian and Moroccan origin respectively [28]. The thujones CT and camphor CT were also found in Egypt and Spain [9].

#### 3.2. Chiral HPLC

TCI-MBS column associated with a polarimetric detection for EO analysis was reported for the first time by El Montassir et al. [10] to detect epimeric thujones and the chirality of the major enantiomer of camphor. The advantages of this method are short time analysis, good detection and separation of the chiral molecules in the EOs without any sample pre-treatment. This method is well adapted to the study of EOs.

The TCI-MBS column was thus used to separate  $\alpha$ - and  $\beta$ -thujone and camphor in the four samples of *AHA*-EOs. For the four samples, the polarimeter clearly detects the presence of (–)- $\alpha$ -thujone, (+)- $\beta$ -thujone and (–)-camphor as prevailing enantiomers. The four HPLC chromatograms were similar even if the area of the peaks change in agreement with relative percentage obtained in GC-MS. A typical chromatogram of *AHA*-EO is presented in [Fig. 1](#). Some non-retained chiral compounds such as  $\alpha$ -pinene, camphene, sabinene,  $\beta$ -pinene and 4-carene were also detected. The other constituents of the crude EOs (achiral and chiral compounds) are present in very low concentration, and give no signal with the polarimeter detector.

#### 3.3. IR and VCD of pure samples

The measured IR and VCD spectra of optically pure (–)- $\alpha$ -thujone, (+)- $\beta$ -thujone and (+)-camphor are presented in [Fig. 2](#). According to the literature [29,30], the absolute configurations of (–)- $\alpha$ -thujone and (+)- $\beta$ -thujone are respectively (1*S*,4*R*,5*R*)-(–)-4-methyl-1-(propan-2-yl)-bicyclo-[3.1.0]-hexan-3-one and (1*S*,4*S*,5*R*)-(+)-4-methyl-1-(propan-2-yl)-bicyclo-[3.1.0]-hexan-3-one respectively. These configurations, which were previously assigned on the basis of chemical correlations, were confirmed herein for the first time using VCD by comparing the corresponding measured and calculated IR and VCD spectra. (+)-Camphor absolute configuration was already determined by VCD and was found to be (1*R*,4*R*) [31].

[Figs. 3–5](#) show IR and VCD spectra of (–)- $\alpha$ -thujone, (+)- $\beta$ -thujone and (+)-camphor in the 1500–1050  $\text{cm}^{-1}$  range. In fact, as VCD and IR spectrum show bands at the same frequencies, VCD bands can be positive or negative band [32]. The assignment of the major bands was done from the calculated spectra and the literature data [29,33]. IR spectra of (–)- $\alpha$ -thujone and (+)- $\beta$ -thujone are quite similar with strong bands at 1458  $\text{cm}^{-1}$  ( $\delta$  CH<sub>2</sub>), 1367  $\text{cm}^{-1}$  (C–H bending), 1240  $\text{cm}^{-1}$  (C–O stretching vibration) and 1174  $\text{cm}^{-1}$  (C–CH<sub>3</sub> stretching vibration). The strong bands at

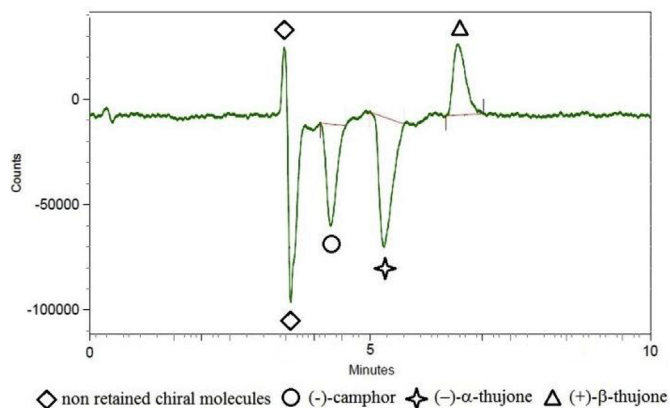


**Fig. 1.** HPLC on TCI-MBS (250 × 4.6 mm) of crude EO1 with polarimetric detection (1 ml min<sup>−1</sup>, 99:1 v/v hexane/2-PrOH, 25 °C).



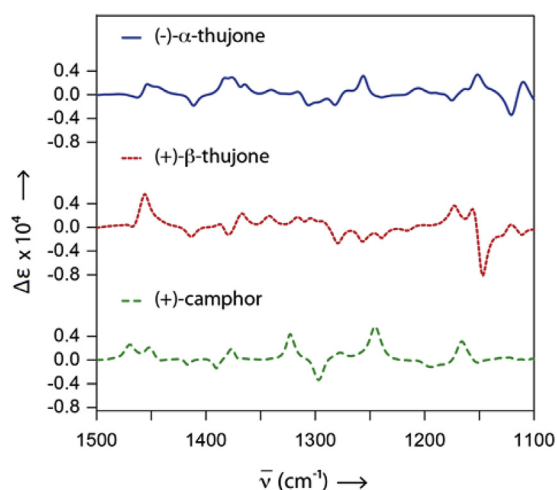


**Fig. 2.** VCD spectra of the three major chiral compounds of AHA-EO. Blue: (–)- $\alpha$ -thujone, red: (+)- $\beta$ -thujone and green: (+)-camphor. (For interpretation of the references to colour in this figure legend, the reader is referred to the web version of this article.)

1450  $\text{cm}^{-1}$  ( $\delta_{\text{asym}} \text{CH}_3$ ), 1417  $\text{cm}^{-1}$  ( $\text{CH}_2$  scissoring), 1390  $\text{cm}^{-1}$  and 1373  $\text{cm}^{-1}$  ( $\delta_{\text{sym}} \text{CH}_3$ ) characterize (+)-camphor IR and VCD spectra (Table S-2). For both, (–)- $\alpha$ -thujone and (+)- $\beta$ -thujone, a satisfying agreement between measured and calculated IR spectra (Figs. 3 and 4) was established. Same agreements were obtained between VCD spectra. Thus, the positive bands at 1456, 1384, 1367, 1256, 1160 and 1110  $\text{cm}^{-1}$  and negative bands at 1411, 1307, 1275 and 1118  $\text{cm}^{-1}$  allowed us to attribute the absolute configuration (1*S*,4*R*,5*R*) to (–)- $\alpha$ -thujone. In the same way, the positive bands at 1458, 1366, 1173 and 1159  $\text{cm}^{-1}$  and negative bands at 1413, 1280, 1257, 1239, 1148 and 1059  $\text{cm}^{-1}$  allowed us to attribute the absolute configuration (1*S*,4*S*,5*R*) to (+)- $\beta$ -thujone. In a mixture, the distinction between two chiral molecules will be possible using VCD only if their spectra are sufficiently different and intense. (–)- $\alpha$ -Thujone, (+)- $\beta$ -thujone and (+)-camphor VCD spectra meet these conditions (Table S-2), so they are good candidates for our study of EOs.

### 3.4. IR and VCD of EOs

The VCD spectra of EO1 and EO4 (Fig. 6) were very similar with a Pearson correlation percentage of 95.7% and present a similar profile as their main constituents: (–)- $\alpha$ -thujone (57.36% and 58.21% respectively). There were some differences between these

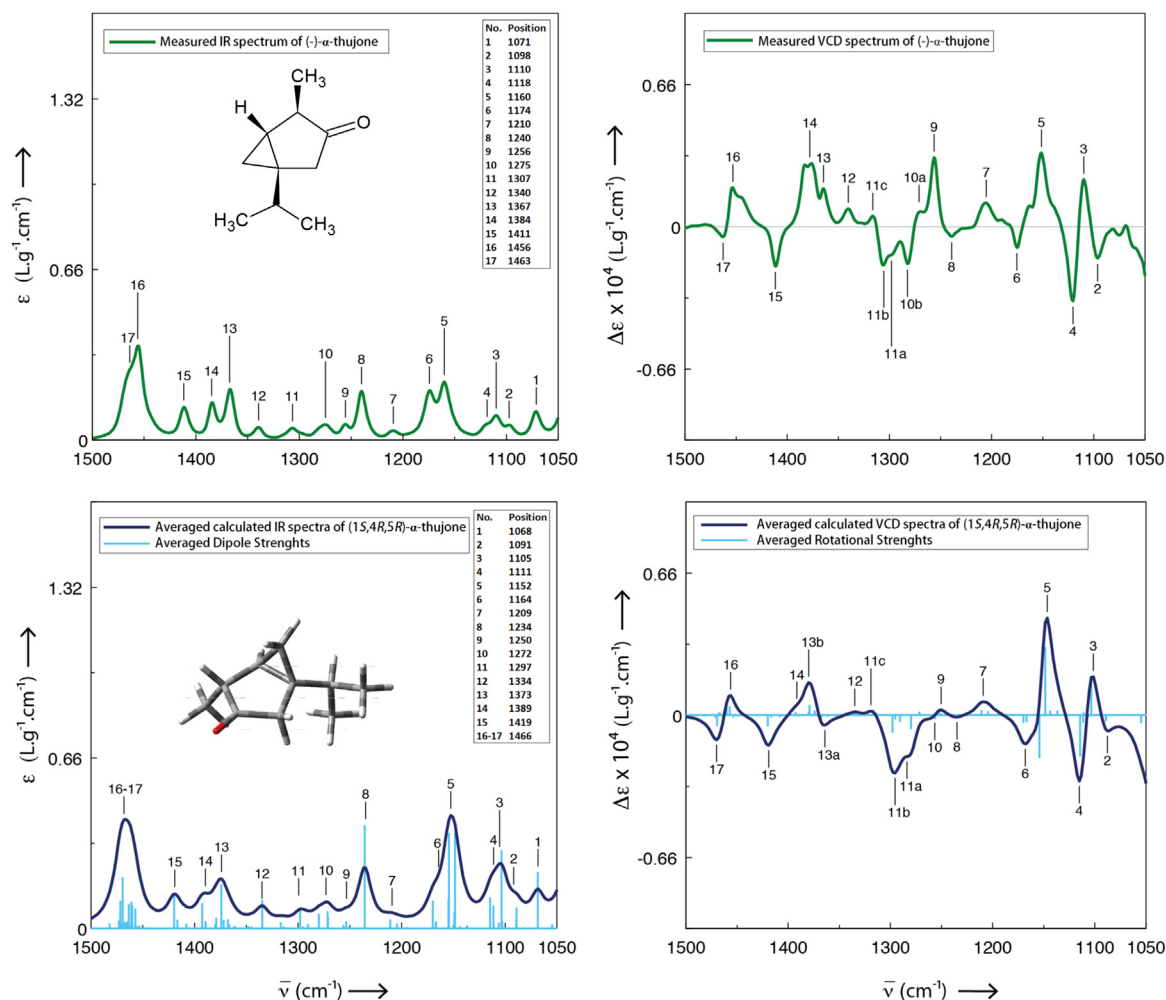


**Fig. 3.** Measured and calculated IR and VCD spectra of (–)- $\alpha$ -thujone. Green: Measured spectra, dark blue: averaged calculated spectra and light blue: averaged dipole strengths. (For interpretation of the references to colour in this figure legend, the reader is referred to the web version of this article.)

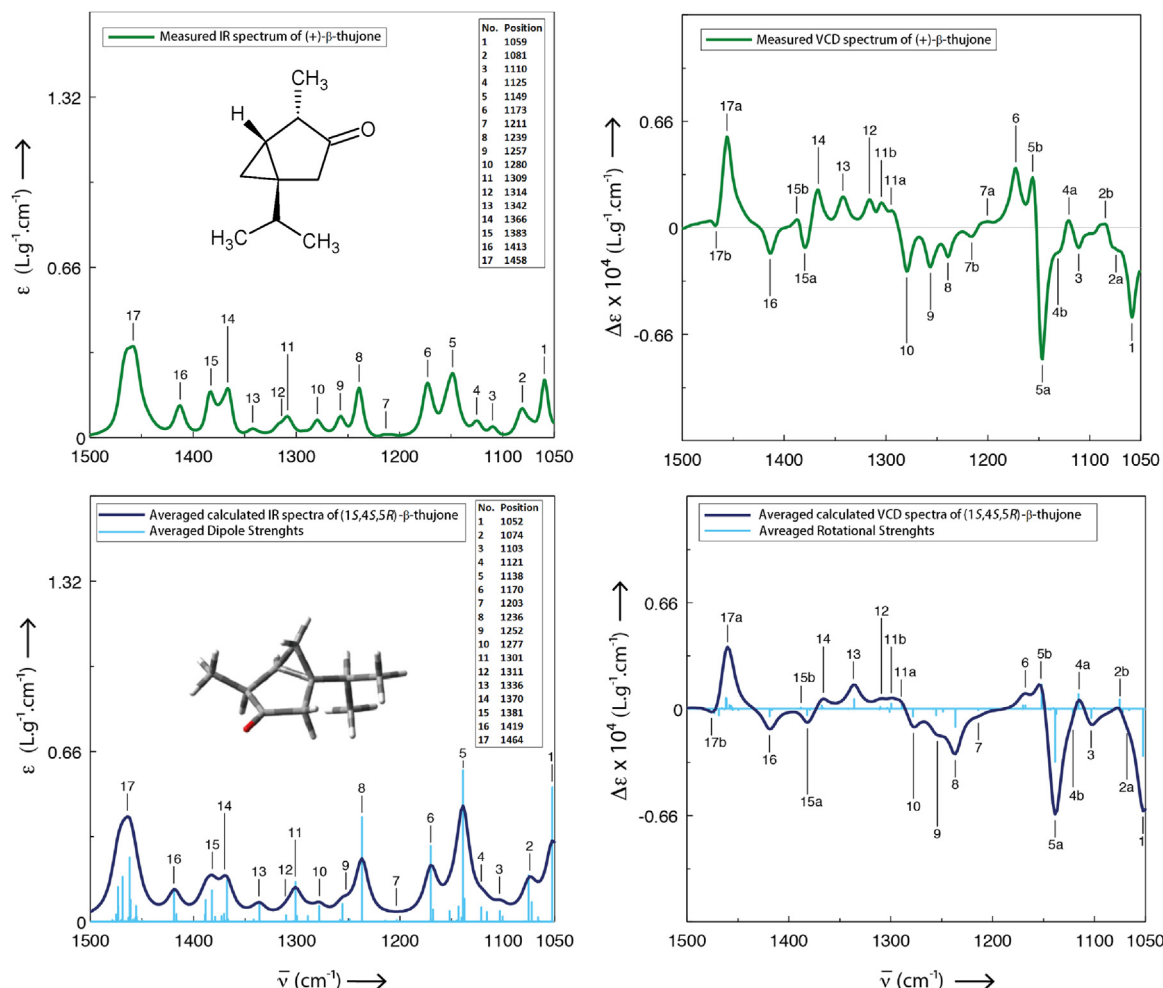


**Fig. 4.** Measured and calculated IR and VCD spectra of (+)-β-thujone. Green: Measured spectra, dark blue: averaged calculated spectra and light blue: averaged dipole strengths. (For interpretation of the references to colour in this figure legend, the reader is referred to the web version of this article.)

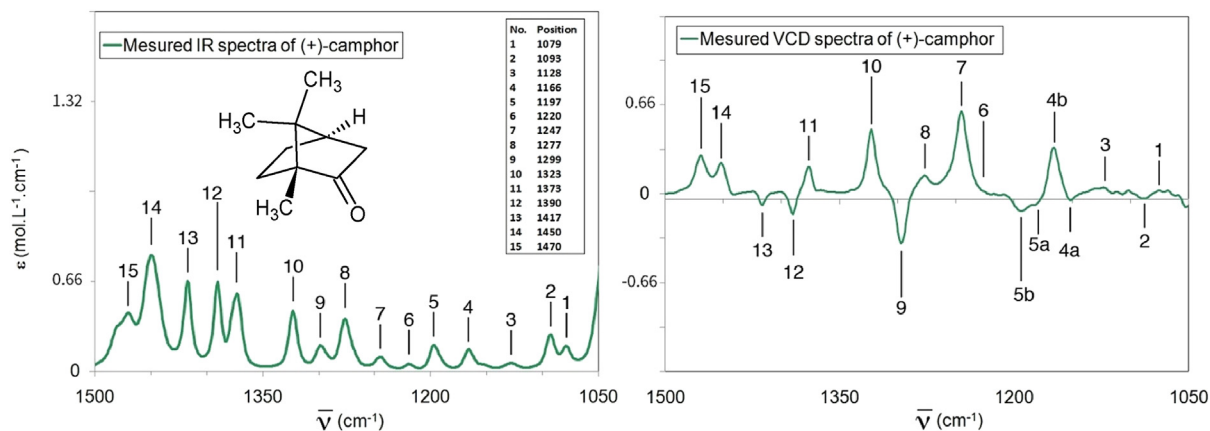


**Fig. 5.** Measured IR and VCD spectra of (+)-camphor.

two spectra in the region 1175–1245  $\text{cm}^{-1}$ . In fact, the band at 1196  $\text{cm}^{-1}$  was most intense for EO1 and the band at 1209  $\text{cm}^{-1}$  characterized EO4 (absent in EO1). The VCD spectrum of EO2 (Fig. 6) characterized by a high content of (–)-α-thujone (35.4% GC) and (+)-β-thujone (25.6% GC), displayed bands at 1457, 1411 and 1160  $\text{cm}^{-1}$  attributed to (–)-α-thujone and at 1411, 1148  $\text{cm}^{-1}$  and

1457  $\text{cm}^{-1}$  (strong band) relative to (+)-β-thujone. The VCD spectrum of EO2 was moderately similar to VCD spectra of EO1 and EO4 with a Pearson correlation percentage of 83.7 and 81.9% respectively. A difference between the VCD spectrum of EO2 and VCD spectra of EO1 and EO4 could be observed in the region 1281–1245  $\text{cm}^{-1}$ : absence of the band at 1256  $\text{cm}^{-1}$  in EO2 which

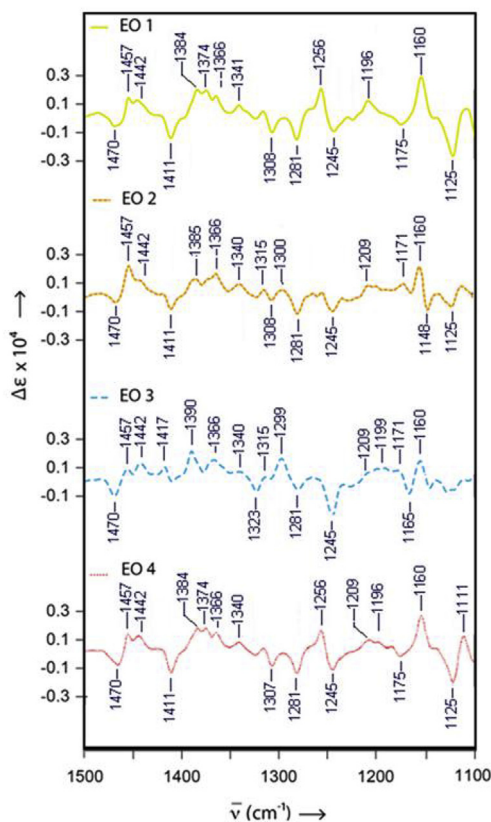


**Fig. 6.** VCD spectra of the four samples of AHA-EOs. Yellow: EO1, orange: EO2, blue: EO3 and red: EO4. (For interpretation of the references to colour in this figure legend, the reader is referred to the web version of this article.)

**Table 1**  
x-Coefficient value from IR and VCD spectra.

Molecules		LSE of VCD/IR spectra			
		EO1	EO2	EO3	EO4
(-)- $\alpha$ -Thujone	$x_1$	0.71/0.72	0.45/0.44	0.26/0.24	0.70/0.69
(+)- $\beta$ -Thujone	$x_2$	0.11/0.11	0.32/0.29	0.13/0.15	0.13/0.12
(+)-Camphor	$x_3$	-0.16/0.15	-0.22/0.21	-0.57/0.45	-0.16/0.16

is typical for (-)- $\alpha$ -thujone (Fig. 3) and presence of the strong band at 1475 cm<sup>-1</sup> in EO2 typical for (+)- $\beta$ -thujone (Fig. 4).

VCD spectrum of EO3 (Fig. 6) was mostly characterized by bands representative of (-)-camphor (1166, 1245, 1299, 1390 and 1470 cm<sup>-1</sup>) since camphor represented 34.5% of the oil (Fig. 5). This result is in accordance with the result of GC (Table S-1) where EO1, 2 and 4 are thujones CT and EO3 is camphor CT. We conclude that IR and VCD spectra of the EOs present similar profiles as their main compounds and that the others minor chiral and achiral molecules do not interfere.

**Table 2**  
GC and LSE ratio of the three major chiral compounds from IR and VCD spectra.

Molecules	% LSE of VCD spectra				% LSE of IR spectra				% GC			
	EO1	EO2	EO3	EO4	EO1	EO2	EO3	EO4	EO1	EO2	EO3	EO4
(-)- $\alpha$ -Thujone	73	46	27	71	73	47	27	71	72.7	45.4	25.3	70.3
(+)- $\beta$ -Thujone	11	33	13	13	11	31	17	12	11.8	32.8	17.6	13.7
(-)-Camphor	16	23	58	16	15	22	56	16	15.5	21.8	57.1	16.0

### 3.5. Spectral reconstruction and prediction

A predictive model was proposed to assign the prevailing enantiomeric form and relative percentage of each major chiral constituent in a mixture solely from the IR and VCD spectra of the pure molecules and EOs. According to the literature and the results we have obtained with the GC-MS and the chiral HPLC, the major chiral molecules in AHA-EOs are (-)- $\alpha$ -thujone, (+)- $\beta$ -thujone and (-)-camphor with 100% of ee. In order to build and validate the predictive model (-)- $\alpha$ -thujone, (+)- $\beta$ -thujone VCD spectra were used, while, on purpose, (+)-camphor VCD spectrum was used instead of (-)-camphor VCD spectrum.

For our AHA-EOs, eq. (5) in 2.6 part can be written:

$$\Delta\epsilon_{EO}(\bar{\nu}_i) = x_1\Delta\epsilon_1(\bar{\nu}_i) + x_2\Delta\epsilon_2(\bar{\nu}_i) + x_3\Delta\epsilon_3(\bar{\nu}_i) + B \quad (12)$$

in which  $\epsilon_1(\bar{\nu}_i)$  means the i'th absorptivities value of (1S,4R,5R)-(-)- $\alpha$ -thujone at the i'th wavenumber,  $\epsilon_2(\bar{\nu}_i)$  means the i'th absorptivities value of (1S,4S,5R)-(+)- $\beta$ -thujone at the i'th wavenumber,  $\epsilon_3(\bar{\nu}_i)$  means the i'th absorptivities value of (1R,4R)-(+)-camphor at the i'th wavenumber and B.

Eq. (12) and S-6 (Supporting Information) were used. The x-coefficients (Table 1, Supporting Information) corresponding to ANOVA analysis were obtained after LSE.

As an example EO1 could be described by polynomial extensions as follow:

for VCD spectra prediction:

$$\Delta\epsilon_{EO}(\bar{\nu}_i) = (0.71)\Delta\epsilon_1(\bar{\nu}_i) + (0.11)\Delta\epsilon_2(\bar{\nu}_i) + (-0.16)\Delta\epsilon_3(\bar{\nu}_i) + B$$

and for IR spectra prediction:

$$\epsilon_{EO}(\bar{\nu}_i) = (0.72)\epsilon_1(\bar{\nu}_i) + (0.11)\epsilon_2(\bar{\nu}_i) + (0.15)\epsilon_3(\bar{\nu}_i) + B'$$

B and B' are the intercept of the models.

The reconstruction method based on LSE from VCD spectra of EO1 gave the following x-coefficients for the 3 compounds investigated: (1S,4R,5R)-(-)- $\alpha$ -thujone ( $x_1 = 0.71$ ), (1S,4S,5R)-(+)- $\beta$ -thujone ( $x_2 = 0.11$ ) and (1R,4R)-(+)-camphor ( $x_3 = -0.16$ ) (Table 1). The sum of the three coefficients equals 0.98. The missing 0.02 are issuing from model errors and minor contributions of other chiral compounds or intermolecular interactions not included in the model. Accordingly LSE of IR spectra, the x-coefficients were found to be:  $\alpha$ -thujone ( $x_1 = 0.72$ ),  $\beta$ -thujone ( $x_2 = 0.11$ ) and camphor ( $x_3 = 0.15$ ). The x-coefficients for the other EOs are given in Table 1. The x-coefficients being very similar from VCD and IR LSE models, it can be safely concluded that within the method precision the three main chiral constituents of EO1 are in nearly optically pure form. The sign associated to an x-coefficient is also quite informative: the occurrence of negative sign associated to an x-coefficient indicates that the actual major enantiomer found in the EO has the opposite configuration to the one introduced into the VCD LSE model. As stated before, the model was built using (1S,4R,5R)-(-)- $\alpha$ -thujone, (1S,4S,5R)-(+)- $\beta$ -thujone and on purpose (1R,4R)-(+)-camphor. The x-coefficients of the two thujones are positive indicating the correctness of the enantiomer choice. The x-coefficient of camphor



is negative indicating that the camphor enantiomer used to build the model is not the prevailing one (Table 1). We used (+)-camphor instead of (–)-camphor intentionally to validate the mathematical model (LSE) and to prove its effectiveness. The occurrence of (–)-camphor is in agreement with the results obtained by chiral HPLC with polarimetric detection. The same approach was done with the infrared spectra using the same pure components, which was recorded at the same time, same solution and same conditions. The results of this calculation are presented in Table 1.

From GC results, (–)- $\alpha$ -thujone (**1**) + (+)- $\beta$ -thujone (**2**) + (–)-camphor (**3**) = 78.9%, 78.0%, 60.8% and 82.7% (Table S-1) of the total composition of the EOs 1, 2, 3 and 4 respectively and (**1/2/3**) are in a ratio of (72.7/11.8/15.5), (45.4/32.8/21.8), (25.3/17.6/57.1), (70.3/13.7/16.0) (Table 2) for EOs 1, 2, 3 and 4 respectively.

LSE can be used to predict the ratio ( $\%x_i$ ) for the three major compounds in the EOs according to eq (13).

$$\%x_i = \frac{x_i \times 100}{\sum_{i=1}^3 |x_i|} \quad (13)$$

These predicted ratios (Table 2) were very close to the ratios given by GC. The best correlations obtained using VCD LSE were observed for EOs 1, 2 and 4. For EO3,  $\%x_i$  were less well correlated: (–)- $\alpha$ -thujone (27%<sub>LSE</sub>, 25.3%<sub>GC</sub>), (+)- $\beta$ -thujone (13%<sub>LSE</sub>, 17.6%<sub>GC</sub>) and (–)-camphor (58%<sub>LSE</sub>, 57.1%<sub>GC</sub>) (Table 2). The best correlations in IR LSE were observed for EOs 1 and 4. For EOs 2 and 3,  $\%x_i$  were less well correlated: (+)- $\beta$ -thujone (33%<sub>LSE</sub>, 32.8%<sub>GC</sub>) for EO2 and (–)- $\alpha$ -thujone (27%<sub>LSE</sub>, 25.3%<sub>GC</sub>) for EO3 (Table 2). In addition, the

LSE percentages from IR and VCD spectra were very close particularly for EOs 1, 2 and 4 (Table 2). Therefore we can conclude that we have one enantiomer with high enantiomeric excess. The output regression models are the simulated IR and VCD spectra, which were compared to the measured spectra (Figs. 7 and 8). A correlation percentage and Pearson coefficients between these spectra had been calculated from the ANOVA analysis (Supplementary materiel). The simulated IR spectra for EOs 1 and 4 present 98% of similarity with the analysis spectra, EO2 present 94% and EO3 present 91% (Table 3). The simulated VCD spectra for EOs 1, 2 and 4 present 98% of similarity with the analysis spectra, EO3 present 94% (Table 3). In summary, The LSE  $x$ -coefficients sign and value allowed to address the prevailing eantiomeric form and molar fraction of enantiomers. The absolute configurations of the prevailing enantiomeric forms in the crude EOs can be assigned since the absolute configuration of the major chiral compounds of AHA-EO were independently determined by comparison of their measured and calculated spectra (Figs. 3 and 4).

#### 4. Conclusion

Different chromatography and spectroscopy techniques were used for the study of AHA-EOs from Algeria and Morocco (GC–MS, chiral HPLC, IR and VCD) with a special attention to their chiral signatures. These EOs were characterized by a large amount of  $\alpha$ -thujone,  $\beta$ -thujone and camphor. The ORS (optical rotation sign) of (–)- $\alpha$ -thujone, (+)- $\beta$ -thujone and (–)-camphor were determined

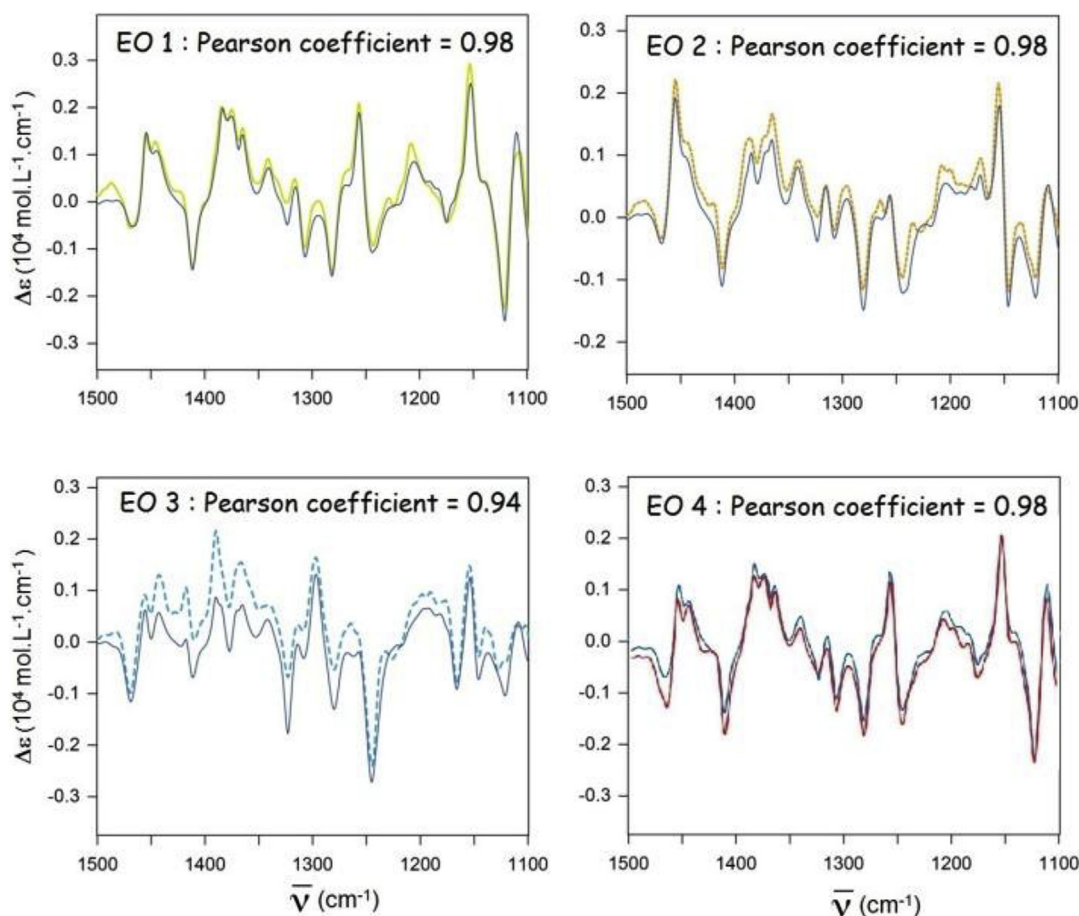


**Fig. 7.** Measured and modeled VCD spectra of EOs. Yellow: EO1, orange: EO2, blue: EO3 and red: EO4. (For interpretation of the references to colour in this figure legend, the reader is referred to the web version of this article.)

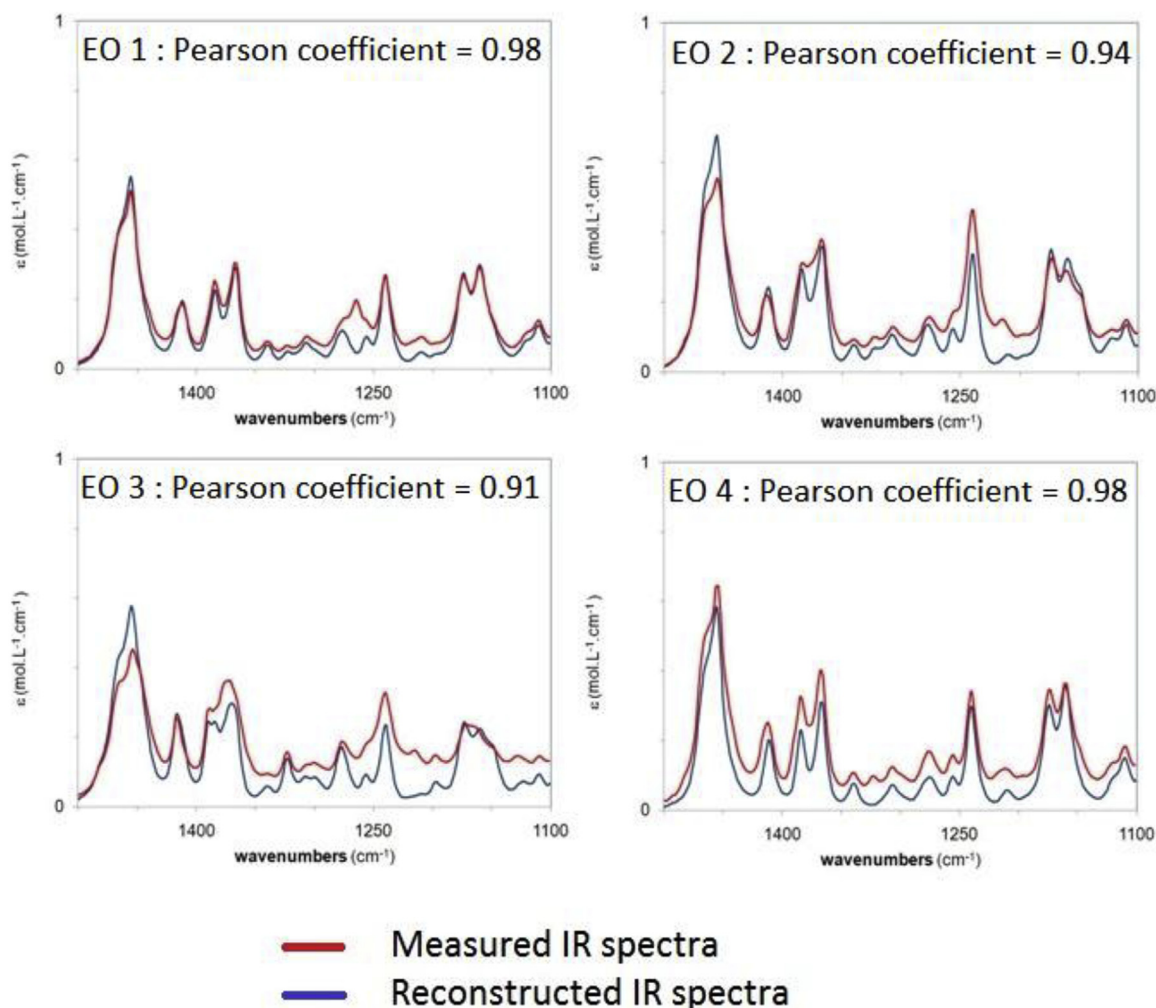


Fig. 8. Measured and modeled IR spectra of EOs.

Table 3

Pearson coefficient obtained from the LSE models using VCD and IR spectra.

Samples	Pearson coefficient from IR spectra	Pearson coefficient from VCD spectra
EO1	0.98	0.98
EO2	0.94	0.98
EO3	0.91	0.94
EO4	0.98	0.98

by enantioselective chiral HPLC with polarimetric detection. Furthermore, the absolute configurations of (–)- $\alpha$ -thujone and (+)- $\beta$ -thujone were determined for the first time by VCD. An original validation method was developed by combining IR, VCD and LSE (least square estimation). The method provided the relative percentage of the three major chiral compounds of *AHA*-EOs, which were very close to those given by GC–MS. More interestingly, the method provided the prevailing enantiomeric form, which can be linked to the absolute configuration of the major chiral constituents when known. The percentages resulting for the LSE of IR and VCD spectra being quite similar, it can be concluded that chiral thujones and camphor were present in the EO as a single enantiomer within the precision of the determination. Reciprocally the comparison of the percentages resulting for the LSE of IR and VCD spectra could be used to detect racemization or non-natural origin of the sample. This mathematical model applied to VCD can be extended to other

EOs or other complex chemical systems, which contain in majority chiral molecules. Further work is underway to validate the method in the case of non-natural mixtures with different enantiomeric compositions.

#### Acknowledgment

CNRS (France) and CNRST (Morocco) are thanked for their support through PIC 24490. European program EMMAG is thanked for a post-doc position (DEM). The ministry of higher education and scientific research (Algeria) is thanked for a post-graduate grant (SM). This work was supported by the computing facilities of the CRCMM “Centre Régional de Compétences en Modélisation Moléculaire de Marseille”.

## References

- [1] M. Zohary, Geobotanical Foundations of the Middle East, Part 1, G. Fischer, France, 1973.
- [2] G. Charalambous, Food Flavors: Generation, Analysis and Process Influence: Generation, Analysis and Process Influence, Elsevier, Amsterdam, 1995.
- [3] H. Mighri, H. Hajlaoui, A. Akrou, H. Najjaa, M. Neffati, Antimicrobial and antioxidant activities of *Artemisia herba-alba* essential oil cultivated in Tunisian arid zone, *Comptes Rendus Chim.* 13 (2010) 380–386.
- [4] S.W. Breckle, Temperate deserts and semi-deserts of Afghanistan and Iran, in: N.E. West (Ed.), Temperate Deserts and Semi-deserts, Ecosystems of the World, vol. 5, Elsevier, Amsterdam, 1983, pp. 271–319.
- [5] H.I. Marriif, B.H. Ali, K.M. Hassan, Some pharmacological studies on *Artemisia herba-alba* (Asso.) in rabbits and mice, *J. Ethnopharmacol.* 49 (1995) 51–55.
- [6] S.M. Salah, A.K. Jäger, Two flavonoids from *Artemisia herba-alba* Asso with in vitro GABAA-benzodiazepine receptor activity, *J. Ethnopharmacol.* 99 (2005) 145–146.
- [7] E. Derwich, Z. Benziane, A. Boukir, Chemical compositions and insecticidal activity of essential oils of three plants *Artemisia* sp: *Artemisia herba-alba*, *Artemisia absinthium* and *Artemisia pontica* (Morocco), *Electron. J. Environ. Agric. Food Chem.* 8 (2009) 1202–1211.
- [8] A. Kadri, I.B. Chobba, Z. Zarai, A. Békir, N. Gharsallah, M. Damak, R. Gdoura, Chemical constituents and antioxidant activity of the essential oil from aerial parts of *Artemisia herba-alba* grown in Tunisian semi-arid region, *Afr. J. Biotechnol.* 10 (2011) 2923–2929.
- [9] S. Salido, L.R. Valenzuela, J. Altarejos, M. Nogueras, A. Sánchez, E. Cano, Composition and infraspecific variability of *Artemisia herba-alba* from southern Spain, *Biochem. Syst. Ecol.* 32 (2004) 265–277.
- [10] D. El Montassir, A. Aamouche, N. Vanthuyne, M. Jean, P. Vanloot, M. Taourirte, N. Dupuy, C. Roussel, Attempts to separate (–)- $\alpha$ -thujone, (+)- $\beta$ -thujone epimers from camphor enantiomers by enantioselective HPLC with polarimetric detection, *J. Sep. Sci.* 36 (2013) 832–839.
- [11] K.H.C. Başer, B. Demirci, N. Tabanca, T. Özek, N. Gören, Composition of the essential oils of *Tanacetum armenum* (DC.) Schultz Bip., *T. balsamita* L., *T. chiliophyllum* (Fisch. & Mey.) Schultz Bip. var. *chiliophyllum* and *T. haradjani* (Rech. fil.) Grierson and the enantiomeric distribution of camphor and carvone, *Flavour Fragr. J.* 16 (2001) 195–200.
- [12] R. Gniłka, A. Szumny, A. Białońska, C. Wawrzęńczyk, Lactones 39. Chemical and microbial synthesis of lactones from (–)- $\alpha$ - and (+)- $\beta$ -thujone, *Phytochem. Lett.* 5 (2012) 340–345.
- [13] H. Schulz, R. Quilitzsch, H. Krüger, Rapid evaluation and quantitative analysis of thyme, origano and chamomile essential oils by ATR-IR and NIR spectroscopy, *J. Mol. Struct.* 661 (2003) 299–306.
- [14] I. Bombarda, N. Dupuy, J.P.L.V. Da, E.M. Gaydou, Comparative chemometric analyses of geographic origins and compositions of lavandin var. Grosso essential oils by mid infrared spectroscopy and gas chromatography, *Anal. Chim. Acta* 613 (2008) 31–39.
- [15] K.W. Busch, M.A. Busch, Chiral Analysis, Elsevier, Amsterdam, 2011.
- [16] A. Krief, M. Dunkle, M. Bahar, P. Bultinck, W. Herrebout, P. Sandra, Elucidation of the absolute configuration of rhizopine by chiral supercritical fluid chromatography and vibrational circular dichroism, *J. Sep. Sci.* 38 (2015) 2545–2550.
- [17] J.M. Batista Jr., B. Wang, M.V. Castelli, E.W. Blanch, S.N. López, Absolute configuration assignment of an unusual homoisoflavanone from *Polygonum ferrugineum* using a combination of chiroptical methods, *Tetrahedron Lett.* 56 (2015) 6142–6144.
- [18] R.D. Singh, T.A. Keiderling, Vibrational circular dichroism of six-membered-ring monoterpenes. Consistent force field, fixed partial charge calculations, *J. Am. Chem. Soc.* 103 (1981) 2387–2394.
- [19] L.A. Nafie, R.K. Dukor, J.R. Roy, A. Rilling, X. Cao, H. Buijs, Observation of Fourier transform near-infrared vibrational circular dichroism to 6150 cm<sup>-1</sup>, *Appl. Spectrosc.* 57 (2003) 1245–1249.
- [20] J. Ren, G.Y. Li, L. Shen, G.L. Zhang, L.A. Nafie, H.J. Zhu, Challenges in the assignment of relative and absolute configurations of complex molecules: computation can resolve conflicts between theory and experiment, *Tetrahedron* 69 (2013) 10351–10356.
- [21] Y. He, B. Wang, R.K. Dukor, L.A. Nafie, Determination of absolute configuration of chiral molecules using vibrational optical activity: a review, *Appl. Spectrosc.* 65 (2011) 699–723.
- [22] P.L. Polavarapu, Determination of the structures of chiral natural products using vibrational circular dichroism, in: N. Berova, P.L. Polavarapu, K. Nakanishi, R.W. Woody (Eds.), *Comprehensive Chiroptical Spectroscopy*, John Wiley & Sons, Inc, 2012, pp. 387–420.
- [23] L.G. Felipe, J.M. Batista, D.C. Baldoqui, I.R. Nascimento, M.J. Kato, Y. He, L.A. Nafie, M. Furlan, VCD to determine absolute configuration of natural product molecules: secolignans from *Peperomia blanda*, *Org. Biomol. Chem.* 10 (2012) 4208–4214.
- [24] J.M. Batista Jr., V. da Silva Bolzani, Determination of the absolute configuration of natural product molecules using vibrational circular dichroism, in: Atta-ur-Rahman (Ed.), *Studies in Natural Products Chemistry*, vol. 41, Elsevier, Amsterdam, 2014, pp. 383–417.
- [25] C. Guo, R.D. Shah, R.K. Dukor, X. Cao, T.B. Freedman, L.A. Nafie, Determination of enantiomeric excess in samples of chiral molecules using fourier transform vibrational circular dichroism spectroscopy: simulation of real-time reaction monitoring, *Anal. Chem.* 76 (2004) 6956–6966.
- [26] H. Schulz, M. Baranska, Identification and quantification of valuable plant substances by IR and Raman spectroscopy, *Vib. Spectrosc.* 43 (2007) 13–25.
- [27] S.A. Van de Geer, Least Squares Estimation, in: Brian S. Everitt, David C. Howell (Eds.), *Encyclopedia of Statistics in Behavioral Science*, vol. 2, John Wiley & Sons, Ltd, Chichester, 2005, pp. 1041–1045.
- [28] G. Vernin, O. Merad, G.M.F. Vernin, R.M. Zamkotsian, C. Párkányi, GC-MS analysis of *Artemisia herba alba* Asso essential oils from Algeria, in: George Charalambous (Ed.), *Developments in Food Science, Food Flavors: Generation, Analysis and Process Influence Proceedings of the 8th International Flavor Conference*, vol. 37, Elsevier, Amsterdam, 1995, pp. 147–205.
- [29] W. Oppolzer, A. Pimm, B. Stammen, W.E. Hume, Palladium-catalysed intramolecular cyclisations of olefinic propargylic carbonates and application to the diastereoselective synthesis of enantiomerically pure (–)- $\alpha$ -thujone, *Helv. Chim. Acta* 80 (1997) 623–639.
- [30] G. Ohloff, G. Uhde, A.F. Thomas, E. Kovats, The absolute configuration of thujane, *Tetrahedron* 22 (1966) 309–320.
- [31] F.J. Devlin, P.J. Stephens, J.R. Cheeseman, M.J. Frisch, Ab initio prediction of vibrational absorption and circular dichroism spectra of chiral natural products using density functional theory: Camphor and Fenchone, *J. Phys. Chem. A* 101 (1997) 6322–6333.
- [32] K.L. Ghatak, A Textbook of Organic Chemistry and Problem Analysis, PHI Learning, Delhi, 2014.
- [33] S. Abbate, L.F. Burgi, F. Gangemi, R. Gangemi, F. Lebon, G. Longhi, V.M. Pultz, D.A. Lightner, Comparative analysis of IR and vibrational circular dichroism spectra for a series of camphor-related molecules, *J. Phys. Chem. A* 113 (2009) 11390–11405.